Simulating the Excited-State Dynamics of Polaritons with Ab Initio Multiple Spawning

Bhaskar Rana,[1,2] Edward G. Hohenstein[1,2], and Todd J. Martínez[1,2]

[1]*Department of Chemistry and The PULSE Institute, Stanford University, Stanford, CA 94305*

[2]*SLAC National Accelerator Laboratory, 2575 Sand Hill Road, Menlo Park, CA 94025*

Abstract

Over the last decade, there has been a growth of interest in polaritonic chemistry, where the formation of hybrid light-matter states (polaritons) can alter the course of photochemical reactions. These hybrid states are created by strong coupling between molecules and photons in resonant optical cavities and can even occur in the absence of light when the molecule is strongly coupled with the electromagnetic fluctuations of the vacuum field. We present a first-principles model to simulate nonadiabatic dynamics of such polaritonic states inside optical cavities by leveraging graphical processing units (GPUs). Our first implementation of this model is specialized for a single molecule coupled to a single photon mode confined inside the optical cavity, but with any number of excited states computed using complete active space configuration interaction (CASCI) and a Jaynes-Cummings type Hamiltonian. Using this model, we have simulated the excited-state dynamics of a single salicylideneaniline (SA) molecule strongly coupled to a cavity photon with the *ab initio* multiple spawning (AIMS) method. We demonstrate how the branching ratios of the photo-deactivation pathways for this molecule can be manipulated by coupling to the cavity. We also show how one can stop the photoreaction from happening inside an optical cavity. Finally, we also investigate cavity-based control of the ordering of two excited states (one optically bright and the other optically dark) inside a cavity for a set of molecules where the dark and bright states are close in energy.

https://doi.org/10.26434/chemrxiv-2023-s7s1t **ORCID:** https://orcid.org/0000-0002-8751-7314 Content not peer-reviewed by ChemRxiv. **License:** CC BY-NC-ND 4.0

I. **Introduction**

There have been many attempts to control molecular processes using strong-fields and coherent control.[1-3] Recently, it has been realized that it is also possible to manipulate the photochemistry of molecules by placing them inside an optical cavity,[4-6] without introducing any chemical modification in the molecules[7, 8] or changing its environment.[9-12] This requires that energy exchange between the molecules and light occurs faster than molecular and/or photonic energy dissipation, often referred to as the strong-coupling limit.[13-15] In this limit, the state of the system can no longer be individually described by the state of light or molecule. These are instead known as polaritons (or dressed states), hybrid states between light and matter.[16-21] Depending upon whether the confined photon mode is strongly coupled with the electronic or vibrational states, there can be exciton-polaritons or vibrational polaritons.[22-29] In this paper, we focus on exciton-polaritons, formed when the photon mode is strongly coupled with the electronic excited states.[30, 31]

The formation of these polaritonic states mixes the photonic and the electronic degrees of freedom, altering the dependence of the polaritonic states on the nuclear degrees of freedom and modifying the potential energy surfaces (PES).[32] Consequently, conical intersections and avoided crossings might move or change their shape in the polaritonic limit, compared to the molecular potential energy surfaces in the absence of a cavity. One can even envision the generation of a completely new set of light induced conical intersections.[33-36] This provides a new route to changing or controlling molecular photochemistry.[4, 18, 19, 33, 34, 37, 38]

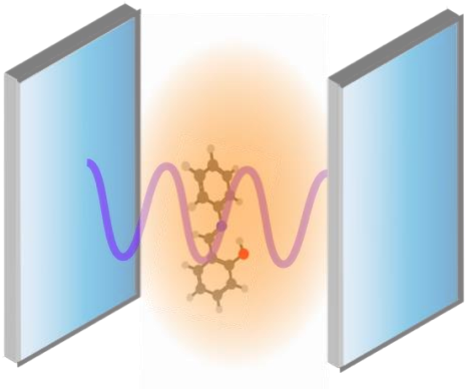

Figure 1. Schematic of an optical cavity where the electronic excited state of a molecule is strongly coupled to a quantized electro-magnetic (EM) field mode.

https://doi.org/10.26434/chemrxiv-2023-s7s1t **ORCID:** https://orcid.org/0000-0002-8751-7314 Content not peer-reviewed by ChemRxiv. **License:** CC BY-NC-ND 4.0

This strong-coupling regime can be realized by letting a molecule interact with a localized light mode confined inside an optical cavity (see Fig.1), where the enhancement of coupling-strength scales as $1/\sqrt{V}$ (V being the photon mode volume).[13, 14, 18] Although strong-coupling can also be achieved by utilizing strong laser fields,[39-42] this can often lead to difficulties because of the increased probability of multiphoton ionization. Within the context of confined optical cavities, strong coupling can be achieved even in the vacuum state (i.e., even in the absence of the external field). Theoretical description of this coupling requires a quantum description of the field.[15, 35] Overall, the optical cavity-based strong-coupling regime has the potential for cleaner controls to modulate photochemical reactivity. The first theoretical description of this quantum field quantization was the Jaynes-Cummings (JC) model[43] which couples a simple two-level electronic system to a single photon mode.

Experimental developments over the last decade made it possible to devise resonant or nano plasmonic cavities for creating such states with strong coupling.[44, 45] Recently, an extension of these experimental advances has become available with a single molecule even at room temperature[16, 46] and also with a microcavity[47] (which increases the lifetime of these interactions[32]). These groundbreaking techniques led to demonstrations of strong coupling to hinder,[48] catalyze,[49] and introduce selective modifications of a chemical reaction.[50] However, these methods of manipulating the strong coupling between molecules and the cavity photon are still in their early stages. Further developments on both experimental and theoretical fronts are required to put these techniques onto solid ground.

The pioneering experimental discoveries have stimulated a plethora of theoretical activity,[17, 32, 35-38, 51-58] which is essential for providing fundamental insights and designing new approaches for applications in this regime. Theoretically, the significant challenges for modeling these states arise from designing approximations to describe coupled nuclear–photonic–electronic states and determining the best representation, i.e. whether to associate the photonic degrees of freedom with the nuclear or electronic wavefunctions.[17, 38, 59-61] Additional theoretical challenges include the proper description of the photonic degrees of freedom and interfacing with a propagation scheme to study the excited-state dynamics, in addition to the usual computational issues associated with photochemical reactions in the absence of a cavity.[59, 61]

Rubio and co-workers[62, 63] developed the first complete quantum method, QEDFT, an extension of time-dependent density functional theory (TD-DFT) to include the photonic degrees

https://doi.org/10.26434/chemrxiv-2023-s7s1t **ORCID:** https://orcid.org/0000-0002-8751-7314 Content not peer-reviewed by ChemRxiv. **License:** CC BY-NC-ND 4.0

of freedom. Further development of this method[17, 60, 64] made it possible to study the cavity-modified properties for both single-molecule and many-molecule cases from first principles.[65] However, this method inherits the limitations of traditional DFT, along with limitations arising from our ignorance of the correct exchange-correlation form for electron-photon coupling. Recently, Haugland et al.[66] developed a formalism based on coupled cluster theory, cavity QED-CC, which can be used for the quantitative description of these polaritonic states. However, for studying excited-state dynamics, the required computational expense presents a significant bottleneck for this method.

Over the last few years, a number of different ways have been developed to deal with the quantum aspect of the nuclear dynamics for such polaritonic states. The multi-configurational time-dependent Hartree (MCTDH) method has been applied to polaritonic systems.[52, 67] Surface hopping methods have been used, with both single-reference and semiempirical multireference electronic structure methods.[61, 68] Semiempirical methods based on real-time nuclear-electronic orbital TD-DFT (RT-NEO-TDDFT) method by Li et al.[69] have also been used.

Despite the emergence of these theoretical and experimental activities in the field, optical cavities are not well-explored in the context of manipulating photochemistry. This demands the development of a model or tool that can be utilized to do fast exploratory excited-state dynamics in a systematic way starting from these polaritonic PES. To build such an efficient model for non-adiabatic polaritonic dynamics, there should be a reasonable balance between accuracy and computational cost. In this regard, although cavity QED-CC[66] offers a more complete and accurate description of the light-matter interactions inside optical cavities, it does not qualify for doing fast exploratory dynamics due to its immense computational cost.

In this work, we present an *ab initio* polariton model, which includes all the electronic, nuclear, and photonic degrees of freedom. The photon-nuclear-electron degrees of freedom are grouped such that the photonic degrees of freedom couple with the electron degrees of freedom rather than the nuclear degrees of freedom. Hence our basis will consist of a product of photon-electron and nuclear basis functions. Our method is most closely related to the model developed by Galego et al.[18] with some modifications. As presented here, our method targets a single molecule coupled with a single cavity photon, but including any number of electronic excited states. Extensions to multiple molecules and/or cavity modes are possible, but left for future work. All the molecular electronic states are computed using the *ab initio* floating occupation molecular

https://doi.org/10.26434/chemrxiv-2023-s7s1t **ORCID:** https://orcid.org/0000-0002-8751-7314 Content not peer-reviewed by ChemRxiv. **License:** CC BY-NC-ND 4.0

orbital-complete active space configuration interaction (FOMO-CASCI) method,[70] allowing for a good description of static correlation (i.e. multireference character in the electronic wavefunction). A Jaynes-Cummings[43] (JC) type Hamiltonian is employed for describing the quantized photonic modes and their interactions with the electronic excited states. The implementation of analytical gradients and non-adiabatic couplings allows us to follow excited-state dynamics on polaritonic potential energy surfaces (PES) using the *ab initio* multiple spawning dynamics[71] (AIMS) method to describe polaritonic surface crossings. Our implementation also leverages graphical processing units (GPU) to achieve the throughput necessary for excited-dynamics simulations. Details of the model are discussed further in the theory section.

Using this model, we have simulated the excited-state dynamics of the salicylidineaniline (SA) molecule and investigated different coupling conditions to manipulate the branching ratio of the two photo-deactivation pathways present in this system. We discuss the conditions under which the presence of the cavity can hinder photoreactions. We also discuss cavity effects on spectra and excited state dynamics in molecules with close-lying electronic states, using trans-butadiene, all trans-octatetraene, and ortho-hydroxybenzaldehyde (OHBA) as examples. These three molecules all have close-lying excited states (one optically bright and the other optically dark) at the S_0 minimum.

II. Theory

In this section, we present our methodology for a single molecule coupled to a single photon mode inside an optical cavity. A Jaynes-Cummings[43] (JC) type Hamiltonian is used for the description of the quantized electromagnetic (EM) mode and the coupling between these modes with the molecular wavefunction. Compared to the free molecule (with no cavity), the total Hamiltonian will now have an additional degree of freedom associated with the confined photon mode. In a typical organic molecule, the energy associated with such strong coupling lies in between nuclear and electronic energies. When it comes to making a choice of coupling the photonic degrees of freedom with either the nuclear degrees of freedom or the electronic degrees of freedom, we have chosen the latter as it leads to well-defined PESs on which the nuclei move,[18] and thus is well-suited for the adoption of nonadiabatic dynamics methods such as AIMS.

https://doi.org/10.26434/chemrxiv-2023-s7s1t **ORCID:** https://orcid.org/0000-0002-8751-7314 Content not peer-reviewed by ChemRxiv. **License:** CC BY-NC-ND 4.0

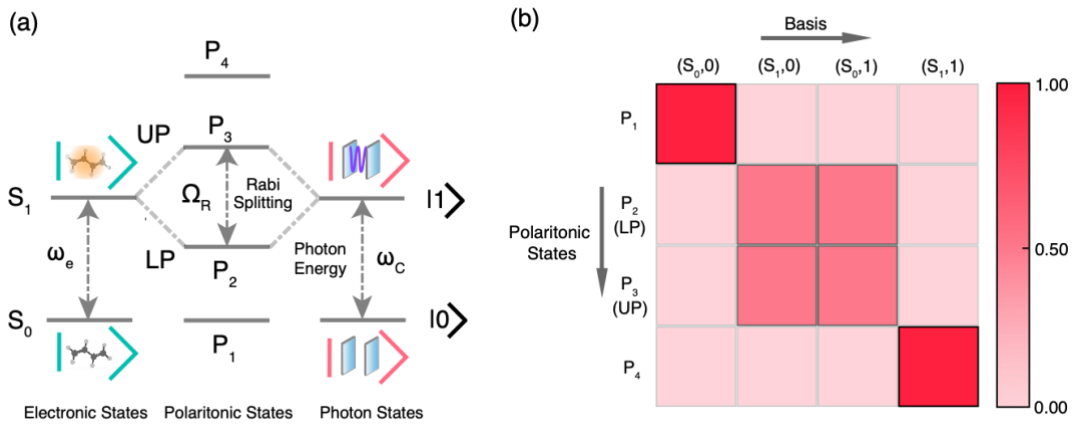

Figure 2. (a) A pictorial representation of our methodology is shown for a two-level system (S_0 and S_1) coupled to a single photon mode ($|0\rangle$ and $|1\rangle$). The strong coupling between $|S_1,0\rangle$ and $|S_0,1\rangle$ states splits the polaritonic energy levels into lower (LP or P_2) and upper (UP or P_3) polaritonic states separated by Ω_R (or Rabi splitting). (b) The contribution of the uncoupled product basis of electronic and photonic wavefunctions to the individual polaritonic states are shown by plotting $|C^i_{n_e,n_{ph}}|^2$ (defined in Eq. 5) at $\omega_e = \omega_c$. As expected, dominant contributions to the LP (P_2) and UP (P_3) states come from both the $|S_1,0\rangle$ and $|S_0,1\rangle$ states.

The total Hamiltonian ($\hat{H}_{total}$) of a polaritonic state is given by,

$$\hat{H}_{total} = \hat{H}_e + \hat{H}_{ph} + \hat{H}_{int} \tag{1}$$

where $\hat{H}_e$ is the standard molecular Hamiltonian, and $\hat{H}_{ph}$ denotes the Hamiltonian for the quantized EM field inside the cavity (neglecting its zero-point energy):

$$\hat{H}_{ph} = \omega_c \hat{a}^\dagger \hat{a} \tag{2}$$

Here, $\hat{a}^\dagger$ and $\hat{a}$ are the creation and annihilation operators for the EM field mode and ω_c is its energy. When this photon energy is resonant with the electronic excitation energy, it is commonly referred to as "zero detuning." We describe the interaction between the electronic state and quantized EM field, $\hat{H}_{int}$, with the Jaynes-Cummings model. Within the dipolar approximation in the Coulomb gauge, the interaction Hamiltonian is given as:

$$\hat{H}_{\text{int}} = g\boldsymbol{\lambda} \cdot \boldsymbol{\mu}^{\mathbf{tr}} \left(\hat{a}^\dagger + \hat{a} \right) \tag{3}$$

Here, the transition dipole moment between two electronic states is denoted as $\boldsymbol{\mu}^{tr}$, $\boldsymbol{\lambda}$ refers to the electromagnetic field polarization unit vector, and g is the coupling strength (or field strength) which depends on the mode volume V as follows:

https://doi.org/10.26434/chemrxiv-2023-s7s1t **ORCID:** https://orcid.org/0000-0002-8751-7314 Content not peer-reviewed by ChemRxiv. **License:** CC BY-NC-ND 4.0

$$g = \sqrt{\frac{\hbar \omega_c}{2\varepsilon_0 V}} \tag{4}$$

Galego et al.[18] estimated the typical field strengths achievable in both the microcavities and plasmonic nanoantennas. In a typical microcavity, one can reach a coupling strength of $g = 1.34 \times 10^{-7}\omega_c^2$ a.u. (where ω_c is in eV).[18] Due to the much lower mode volume (V) accessible in plasmonic nanoantennas,[72] these can achieve much larger coupling of $g = 3.72 \times 10^{-4}\omega_c^2$ a.u. (ω_c is in eV).[18] We have used these typical coupling strengths for all the molecules discussed in the current work (see Table S1). Like the JC model, we use the rotating wave approximation and neglect the permanent dipole and dipole self-energy contributions.

We first compute the adiabatic electronic state by diagonalizing $\hat{H}_e$ with any electronic structure method. Then, the products of these adiabatic electronic states and photonic wavefunctions (known as Fock states) are used as a basis for finding the corresponding polaritonic states. This basis is commonly known as the adiabatic-Fock basis. To differentiate these uncoupled products from the bare electronic states, we denote these states as $|n_e(R),n_{ph}\rangle$ $\left(\equiv \left|n_e(R)\right\rangle \otimes \left|n_{ph}\right\rangle\right)$. Here, n_e carries the index for electronic states (such as S_0, S_1, and so on), whereas n_{ph} is the index for the photon occupation number (which is limited to 0 and 1 in our case). On the other hand, the bare electronic states are represented as $|S_0\rangle$ and $|S_1\rangle$. The polaritonic eigenstates,

$$\left|P_i\right\rangle = \sum_{n_e,n_{ph}} C^i_{n_e,n_{ph}} \left|n_e,n_{ph}\right\rangle \tag{5}$$

are obtained by diagonalizing $\hat{H}_{total}$ (see Eq. 1) in the adiabatic-Fock basis. $C^i_{n_e,n_{ph}}$ are the resulting coefficients for the i-th polaritonic state in the $|n_e,n_{ph}\rangle$ basis.

Fig. 2 depicts a simplified representation of our methodology for a two-level system ($|S_0\rangle$ and $|S_1\rangle$) coupled to a single cavity mode ($|0\rangle$ and $|1\rangle$). In this case, the basis will be composed of $|S_0,0\rangle$, $|S_1,0\rangle$, $|S_0,1\rangle$, and $|S_1,1\rangle$ electronic-photonic products. If the photon energy (ω_c) is resonant with the energy gap between S_0 and S_1 (ω_e) inside an optical cavity, $|S_1,0\rangle$ and $|S_0,1\rangle$ will strongly couple with each other to form two completely new states which are known as the lower-polaritonic state (LP) and the upper-polaritonic state (UP) (see Fig. 2a). The energy gap between these LP and UP states is often referred to as the Rabi splitting (Ω_R), which is a measure of the rate of energy exchange between the electronic and photonic mode (see Fig. 2a). The new polaritonic states

https://doi.org/10.26434/chemrxiv-2023-s7s1t **ORCID:** https://orcid.org/0000-0002-8751-7314 Content not peer-reviewed by ChemRxiv. **License:** CC BY-NC-ND 4.0

(denoted as P_i), written as a linear combination of the uncoupled electron-photon product basis functions, are shown in Fig. 2b. As expected, both the LP and UP states are formed from a strong coupling between $|S_1,0\rangle$ and $|S_0,1\rangle$. The extension of this method to include any number of electronic excited states in the uncoupled product basis ($|n_e,n_{ph}\rangle$) is straightforward.

For the computation of the electronic excited states, we used the FOMO-CASCI method in this work but other choices are possible and require no significant alteration to the formalism. We also have made use of the highly efficient graphical processor unit (GPU) based implementations of the analytical gradients[73] and non-adiabatic coupling[74] matrix elements for FOMO-CASCI. Additionally, analytic derivatives of the FOMO-CASCI dipole matrix have been implemented with GPU acceleration; our formulation of this quantity closely parallels that of the non-adiabatic coupling vector,[74] but requires nontrivial solutions of coupled-perturbed configuration interaction equations. The energies, analytic gradients, and analytic nonadiabatic coupling vectors of this model are implemented in a locally modified version of the TeraChem[75] electronic structure package. This makes it possible to simulate the excited-state dynamics using the AIMS method starting from these strongly coupled polaritonic PES.

III. Results and Discussion

In this section, we explore some proof-of-concept applications employing the polariton model discussed above. In Section IIIA, we investigate how the photochemistry of a single salicylidineaniline (SA) molecule changes inside an optical cavity compared to the bare case scenario. Through the simulation of the excited-state dynamics under various coupling conditions, we elucidate how the branching ratios of the photo-deactivation pathways for this molecule can be modified by coupling to the cavity light mode. In Section IIIB, we discuss the cavity effects in molecules with close-lying electronic excited states, using trans-butadiene, all trans-octatetraene, and OHBA as examples.

A. Excited-state dynamics of a single SA molecule inside an optical cavity

First, we have applied our methodology to investigate the excited-state dynamics of the aromatic Schiff base salicylideneaniline (SA) (shown in Fig. 3) in the strong-field regime. SA is a molecule which exhibits excited-state intramolecular proton transfer (ESIPT) upon photoexcitation. The experimental investigation of excited-state dynamics based on spectroscopic measurements demonstrated the existence of two internal-conversion pathways for this molecule,[76-78] as depicted

https://doi.org/10.26434/chemrxiv-2023-s7s1t **ORCID:** https://orcid.org/0000-0002-8751-7314 Content not peer-reviewed by ChemRxiv. **License:** CC BY-NC-ND 4.0

in Fig. 3a. Theoretical studies[79, 80] on the free molecule agree on the dominant decay pathway being ESIPT with some of studies[80, 81] suggesting the presence of a secondary deactivation pathway involving rotation around the central carbon-nitrogen bond (C=N) which prevents the proton transfer from happening. Hohenstein and co-workers[81] studied the excited-state dynamics of this system by carrying out AIMS simulations using FOMO-CASCI wave functions with embedding corrections[82] from density functional theory (DFT) and provided the first theoretical estimation of the branching ratio of these two photo-deactivation pathways. In that study, 80% of the excited population is found to undergo proton transfer, leading to a metastable state on S_1. The remaining 20% of the population goes through a twisting motion around the C=N bond and does not lead to proton transfer. This population quickly (within ≈300fs) decays to the ground state via a twisted minimum energy conical intersection (MECI).

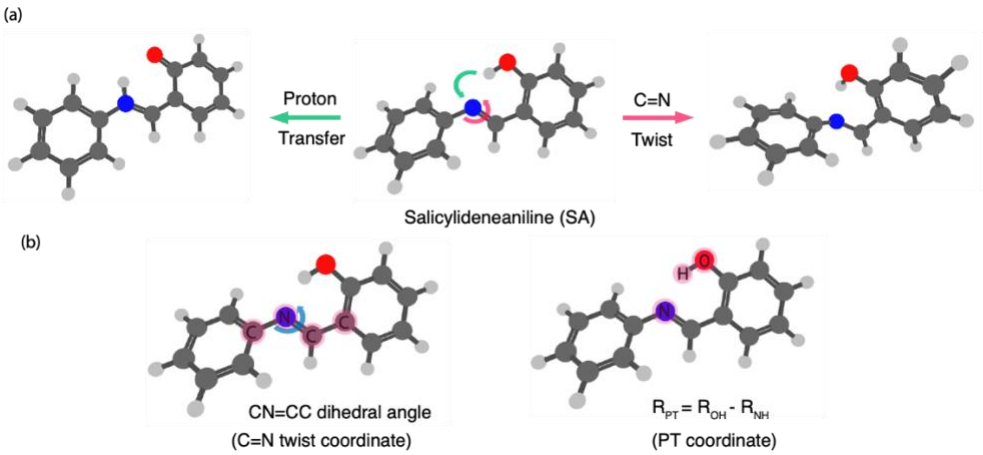

Figure 3. (a) Two possible photo-deactivation pathways of the salicylideneaniline (SA) molecule. The dominant pathway shows the excited state proton transfer (ESIPT). The secondary pathway is associated with a twist around the C=N bond which frustrates the proton transfer. (b) Reaction coordinates are defined for the C=N twist pathway and the PT pathway, respectively.

Given that the excited-state dynamics of the bare SA molecule are already well-established and well-behaved with FOMO-CASCI (the same method is used in our polariton model for computing the excited states) and given the excited-state dynamics lead to two different photoproducts, this molecule represents an interesting case to examine the effect of placing a molecule inside an optical cavity by employing our *ab initio* polariton model. Moreover, the initial conditions that lead to different photoproducts in the bare case are also available separately. By

https://doi.org/10.26434/chemrxiv-2023-s7s1t **ORCID:** https://orcid.org/0000-0002-8751-7314 Content not peer-reviewed by ChemRxiv. **License:** CC BY-NC-ND 4.0

reusing those initial conditions for the polaritonic case, we can easily compare the dynamics with and without a cavity to determine the influence of the polaritonic mixing.

In the following, we focus on elucidating the variations of the branching ratios and the PT timescale for this molecule as a function of the coupling strength inside an optical cavity. The coupling conditions to trap the photoexcited SA molecule around the FC geometry are also explored in detail. In other words, taking this molecule as an example, we have demonstrated the amount of flexibility and control that this strong-field regime offers to modify the photochemical properties.

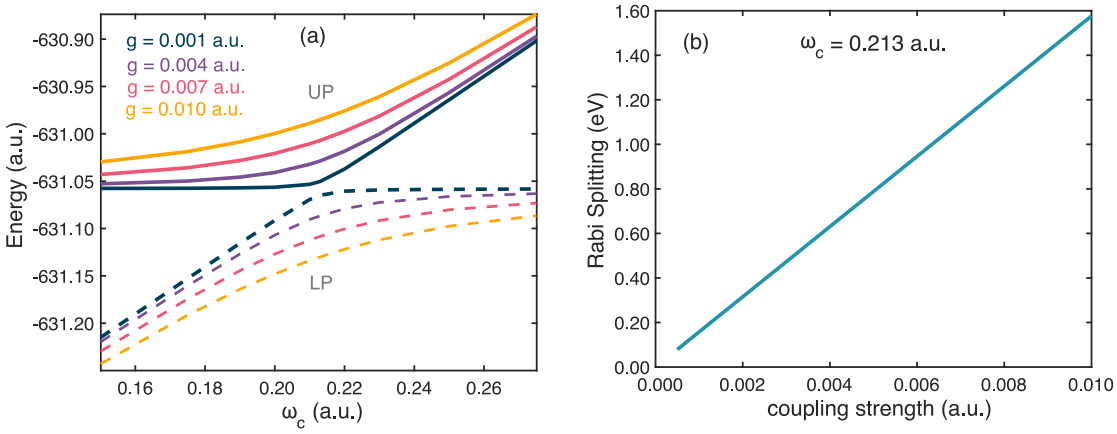

Figure 4. (a) Variation of the energies corresponding to the UP and LP states as a function of coupling strength (g) and photon energy (ω_c) and (b) Rabi splitting (Ω_R) as a function of coupling strength (g) for salicylideneaniline (SA) molecule inside the optical cavity.

Calculations on the SA molecule at the FC geometry with various coupling strengths were used to find suitable cavity parameters for this system. The electronic structure is modeled with FOMO-(2,2)-CASCI/6-31g** with an embedding correction computed using the ωPBEh functional, analogous to the previous simulations of the bare molecule.[81] The Gaussian broadening parameter for the FOMO-CASCI method is 0.075 a.u. and the ω parameter for the DFT correction is 0.200 a.u.

Fig. 4a plots the energies of the LP and UP states as a function of the coupling strength (g) and photon energy (ω_c). The electromagnetic field polarization unit vector is taken to be aligned along the transition dipole moment associated with the $S_0 \rightarrow S_1$ transition at the FC geometry. The Rabi splitting (Ω_R) (see the definition in Fig. 2a), which represents the energy difference between the UP and LP states at zero detuning, is plotted in Fig. 4b as a function of coupling strength. The

https://doi.org/10.26434/chemrxiv-2023-s7s1t **ORCID:** https://orcid.org/0000-0002-8751-7314 Content not peer-reviewed by ChemRxiv. **License:** CC BY-NC-ND 4.0

range of coupling strengths examined is guided by the largest coupling strength expected in plasmonic nanoantennas (0.013 a.u., see Table S1).

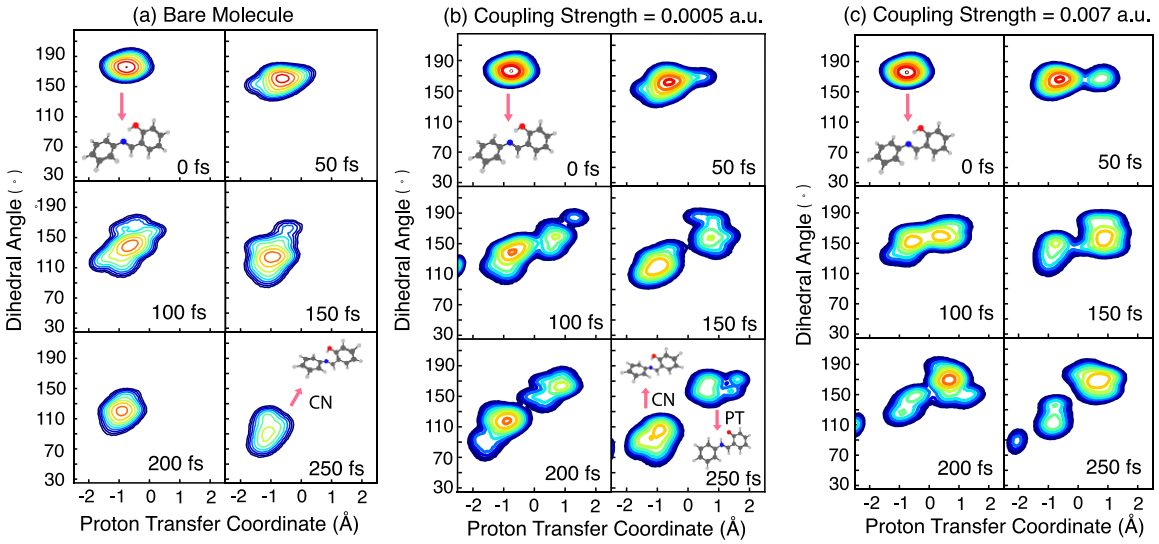

Figure 5. AIMS nuclear density plots along the two essential degrees of freedom (defined in Fig. 3b) are shown for the trajectories initiated from initial conditions which do not lead to proton transfer with (a) the bare molecule, (b) a coupling strength of 0.0005 a.u., and (c) a coupling strength of 0.007 a.u.

The excited-state dynamics inside a cavity are simulated using the AIMS method with two electronic states (S_0 and S_1) coupled with a single cavity-photon (see Fig. 2a). The energy of the confined photon mode (ω_c) is chosen to be resonant with the energy gap between S_0 and S_1 states at the FC geometry. The electromagnetic field polarization unit vector ($\boldsymbol{\lambda}$) is aligned along the direction of the transition dipole moment ($\boldsymbol{\mu}^{tr}$) between S_0 and S_1 states at the FC geometry. Following this setup, the AIMS trajectories were then propagated for 250 fs with a time step of 20 a.u. with varying coupling strengths. For each coupling strength, we have run simulations with 30 different initial conditions leading to ESIPT in the bare molecule and another separate 30 initial conditions where it does not lead to PT. This allows us to compute the effect of the cavity on branching ratios with a small number of trajectories. All these simulations are initiated from the LP state (or P_2 in this case).

https://doi.org/10.26434/chemrxiv-2023-s7s1t **ORCID:** https://orcid.org/0000-0002-8751-7314 Content not peer-reviewed by ChemRxiv. **License:** CC BY-NC-ND 4.0

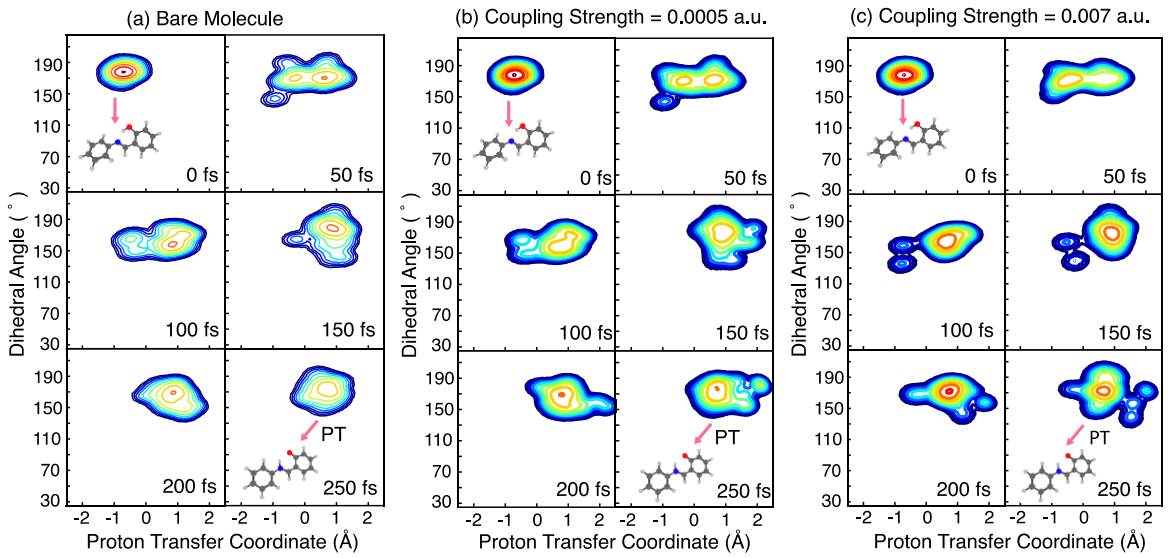

Figure 6. AIMS nuclear density plots along the two essential degrees of freedom (defined in Fig. 3(b)) are shown for the trajectories initiated from a PT-bound initial conditions with (a) the bare molecule, (b) a coupling strength of 0.0005 a.u., and (c) a coupling strength of 0.007 a.u.

The two essential degrees of freedom associated with the excited-state dynamics for this molecule are depicted in Fig. 3b. For the dominant PT pathway, the reaction coordinate (R_{PT}) is defined as the difference between the O–H and N–H bond lengths (see Fig. 3b). To track the secondary pathway associated with a C=N twist, we follow a dihedral angle around the C=N bond (CN=CC) as shown in Fig. 3b. At the FC geometry, the dihedral angle is 180° and the PT coordinate is ≈ -1Å. Trajectory basis functions (TBFs) that undergo proton transfer (PT coordinate evolving to ≈1Å) typically do so very quickly (within 100fs), before any significant twisting motion (dihedral angle remains within 40° of planarity) takes place.[82] Once the twisting angle goes beyond 40° of planarity, proton transfer no longer occurs[82] and instead the molecule undergoes internal conversion through a twisted MECI. We followed the dynamics in the cavity for up to 250 fs, monitoring these two coordinates (see Figs. 5b-c and Figs. 6b-c) for two different coupling strengths. The AIMS nuclear densities are calculated by using a Monte-Carlo algorithm[82-84] averaged over 30 trajectories for each case. A detailed description of this procedure has been explained previously.[83]

Fig. 5 depicts the time evolution of the nuclear wave packets for the TBFs started from the bare molecule initial conditions that undergo C=N twist (see Fig. 5a). The dynamics of these TBFs is significantly affected by the coupling to a cavity photon. With a coupling strength as low as

https://doi.org/10.26434/chemrxiv-2023-s7s1t **ORCID:** https://orcid.org/0000-0002-8751-7314 Content not peer-reviewed by ChemRxiv. **License:** CC BY-NC-ND 4.0

0.0005 a.u. (corresponding to a Ω_R value of around 100 meV), the TBFs bifurcate from C=N twist to a combination of PT and C=N twist pathways (Fig. 5b). The C=N twist pathway remains the dominant path (≈33% converts to PT). However, with a larger coupling strength value of 0.007 a.u. (Fig. 5c), around 73% of the TBFs which led to C=N twist in the bare case instead undergo proton transfer within 250 fs. In contrast, the TBFs which undergo proton transfer in the bare molecule are unaffected by the cavity mode, for both investigated coupling strengths. These still show PT inside a cavity (see Fig. 6). Therefore, coupling the SA molecule with a single cavity-photon increases the branching ratios in favor of the PT pathway, leading to more than 80 percent of the photoproduct undergoing proton transfer.

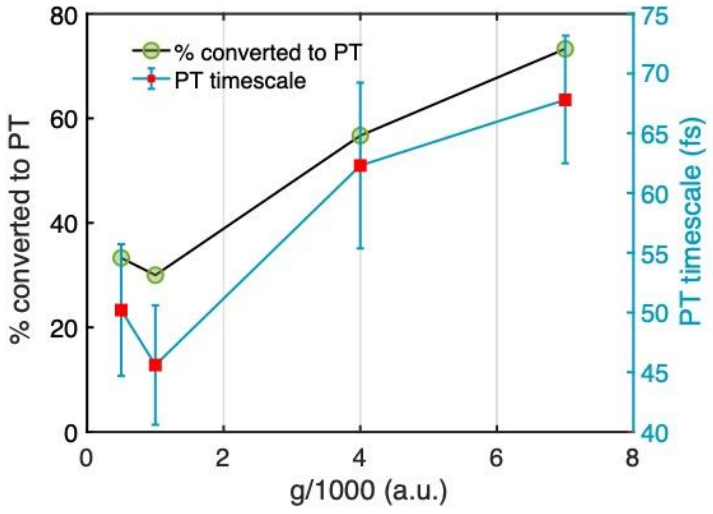

Figure 7. Percentage conversion of the C=N twist pathway to a proton transfer pathway and average proton transfer timescale along with the error bar (averaged over all the TBFs which undergo PT) are shown.

A variation of the branching ratios and the time scales of the proton-transfer are plotted as a function of coupling strengths in Fig. 7. The PT timescales are averaged over all TBFs which undergo PT. The percent conversion of a C=N twist pathway to a PT one increases with coupling strength (as noticed in Fig. 5 and Fig. 6). With a coupling strength of 0.007 a.u. (the largest in our simulations), we can convert nearly 75% of the C=N twist pathway to the PT pathway, which corresponds to a branching ratio of 95:5 for the PT vs. C=N twist pathway (compared to 80:20 in the bare case). We did not investigate larger coupling strengths since the maximum coupling strength that can be achieved experimentally is limited to the mode volume of the cavity mode. These results demonstrate that the optical cavity can manipulate the branching ratio of the two

https://doi.org/10.26434/chemrxiv-2023-s7s1t **ORCID:** https://orcid.org/0000-0002-8751-7314 Content not peer-reviewed by ChemRxiv. **License:** CC BY-NC-ND 4.0

pathways for the excited-state dynamics of the SA molecule (compared to the bare molecule with no optical cavity).

The timescale of PT tends to lengthen with increasing coupling strengths (as shown in Fig. 7). To explain the dependence of PT timescale and branching ratio on coupling strength, we have computed the two-dimensional potential energy surfaces (2D-PES) for the lower polaritonic state (LP) along the CN=CC dihedral angle and the O-H bond length (represented as r_{OH}). These PESs were generated through a set of constrained optimizations fixing the CC=NC dihedral angle and r_{OH} for g = 0.0005 a.u. and g = 0.007 a.u. The 2d PESs are compared in Fig. S1.

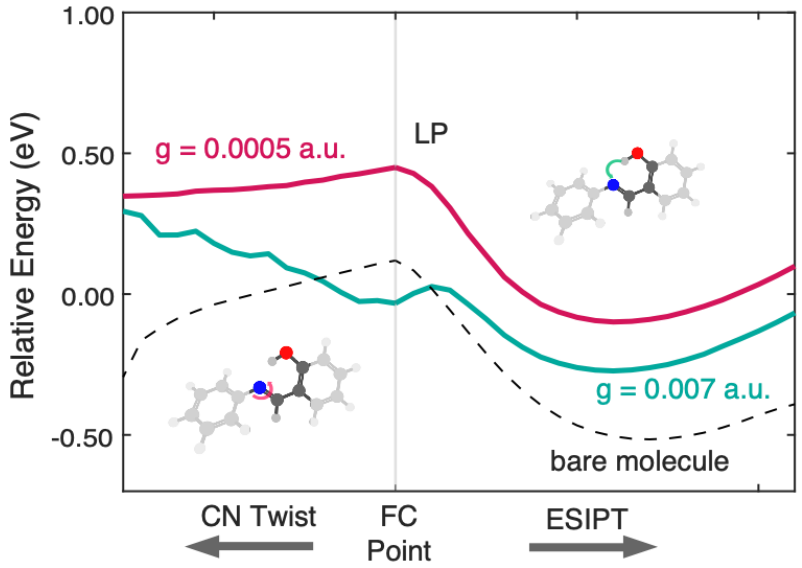

Figure 8. Cuts through the optimized potential energy surfaces (PES) around the FC point relaxed with respect to the lower-polaritonic (LP or P2) state are shown along the O-H bond length (for the PT pathway) and the CC=NC dihedral angle (for the CN twist pathway). The energies are computed for g = 0.0005 a.u. and g = 0.007 a.u. by doing constrained optimization with FOMO-(2,2)-CASCI/6-31G** on the P2 surface. The dashed curve represents the cuts for the bare molecule where the constrained optimizations are done on the bare molecule S_1 surface using the same level of theory.

One-dimensional cuts of the PES along these two degrees of freedom are plotted in Fig. 8 for both coupling strengths and compared to the bare molecule. In the bare molecule (dashed line in Fig. 8), both ESIPT and CN twist pathways are feasible. Both pathways remain feasible when the molecule is in a cavity with the smaller g value (the red curve in Fig. 8), although one already sees that the CN twist is less favorable (slope is less steep going from the FC point to the CN twisted

https://doi.org/10.26434/chemrxiv-2023-s7s1t **ORCID:** https://orcid.org/0000-0002-8751-7314 Content not peer-reviewed by ChemRxiv. **License:** CC BY-NC-ND 4.0

form). For the larger coupling strength (g = 0.007 a.u.), motion along the C=N twist is disfavored (primarily because the FC point has been stabilized on the lower polaritonic state). This makes ESIPT even more dominant. The longer timescale for proton transfer with larger coupling strength can be explained by the emergence of a small energy barrier near the FC point along the PT coordinate with g = 0.007 a.u. (which was absent with g = 0.0005 a.u.).

The results discussed so far for the SA molecule are focused on the case where the cavity-photon is resonant with the energy gap between the S_0 and S_1 states (also known as "zero-detuning"). Therefore, now, we investigate the effect of lowering or raising the photon energy on the excited-state dynamics for the SA molecule. We simulated the polaritonic excited-state dynamics with AIMS using a photon energy of 0.175 a.u. (4.76 eV) and 0.250 a.u. (6.80 eV), bracketing the resonant photon energy of 0.212 a.u. (5.77 eV). The corresponding AIMS nuclear density plots are shown in Fig. 9 (ω_c = 0.175 a.u.) and Fig. S2 (ω_c = 0.250 a.u.) for both the PT and C=N twist pathways. When the photon energy is off-resonant to the blue, the cavity has little effect on the dynamics compared to the bare molecule (see Fig. S2). However, when the photon energy is off-resonant to the red, the effect of the cavity on the dynamics is even more pronounced than the resonant case (Fig 9). The SA molecule excited to the LP state is trapped around the FC geometry on the 250 fs timescale of our AIMS dynamics. Only a very small amount of proton transfer is observed and the C=N twist is almost undetectable. In this case, detuning the photon energy below resonance arrests the photoreaction.

This observation seems to be very surprising at first glance, but can be understood by comparing the character of (S_0,1) and (S_1,0) (see Fig. 2 for the definitions) on the lower polaritonic (LP) state. When the photon energy is resonant with S_1, or off-resonant with higher energy, the LP state is dominated by S_1 character. However, when the photon energy is off-resonant with lower energy, the (S_0,1) state becomes lower in energy compared to the (S_1,0) state. Thus, the LP state (P_2 state in Fig. 2) is largely characterized by the shape of the (S_0,1) state, and this helps to trap the SA molecule in the LP states and stop the photoreaction from happening. This scenario can be created for any molecule photo-excited to the LP state. Although it does not lead to an exciting outcome in the present case, the detuning can have an effect in selectively trapping a photoproduct in other scenarios.

https://doi.org/10.26434/chemrxiv-2023-s7s1t **ORCID:** https://orcid.org/0000-0002-8751-7314 Content not peer-reviewed by ChemRxiv. **License:** CC BY-NC-ND 4.0

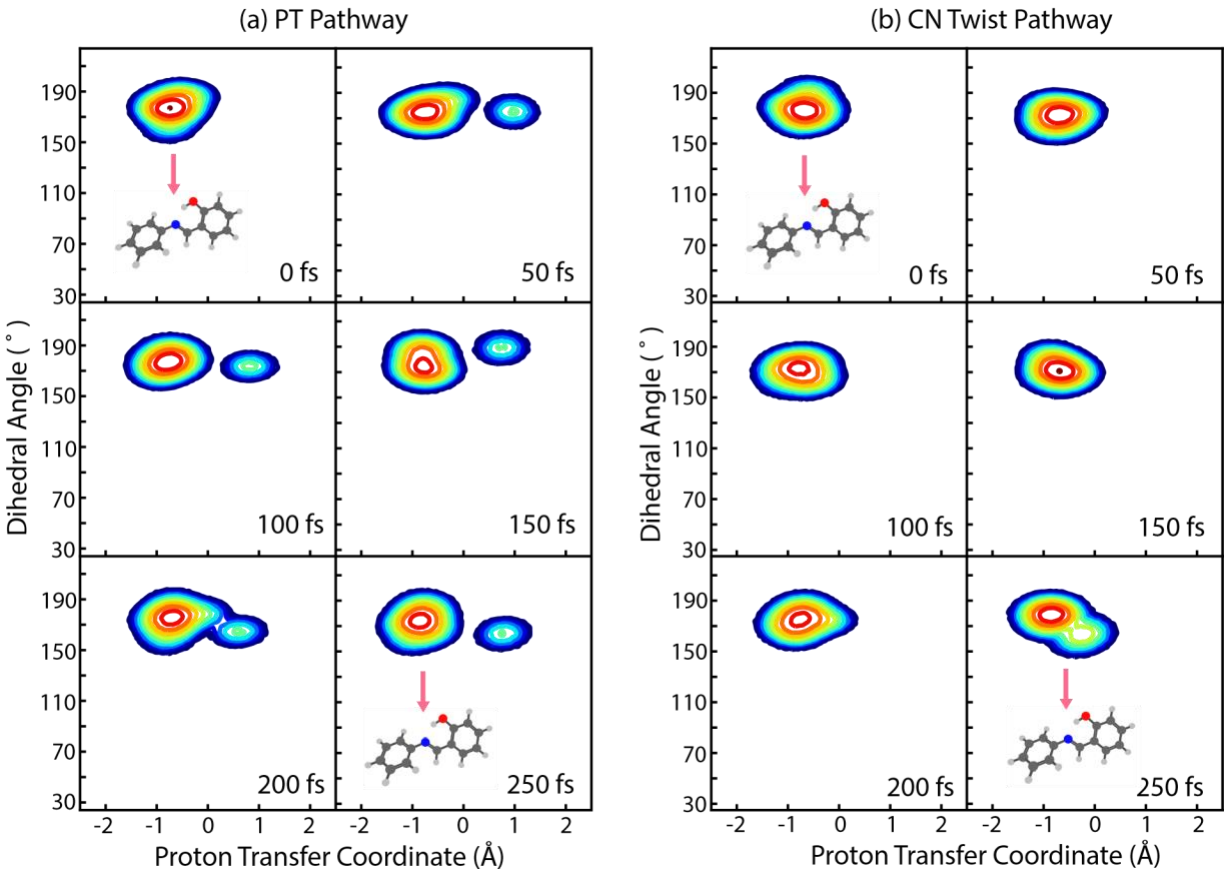

Figure 9. AIMS nuclear density plots are shown for both the (a) PT pathway and (b) C=N twist pathway with a photon energy of 0.175 a.u. (whereas the resonant photon energy is 0.212 a.u.). Using these coupling conditions, one can trap the photo-excited SA molecule in the P_2 (or LP) state for the 250 fs timescale of our simulations.

B. Cavity-induced modifications of the energy ordering

Up to this point, cavity-induced effects on the excited-state dynamics have been studied for a single-molecule which can be described as a two-state model (just like the JC model). For the next part of this work, we apply our model to a set of molecules (all-*trans* butadiene, all-*trans* octatetraene, and *o*-hydroxybenzaldehyde) that require three electronic states to describe the polaritonic states adequately. In these molecules, there are close-lying optically bright and optically dark excited states. Selective coupling of the optically bright states to the cavity-photon enables the use of cavity coupling to manipulate the ordering of bright and dark states (which could have significant effects on the excited state dynamics). We do not simulate excited state dynamics

https://doi.org/10.26434/chemrxiv-2023-s7s1t **ORCID:** https://orcid.org/0000-0002-8751-7314 Content not peer-reviewed by ChemRxiv. **License:** CC BY-NC-ND 4.0

on these molecules in this work (leaving that for future studies), but we do demonstrate the role of coupling to the optical cavity on the electronic states at the FC point.

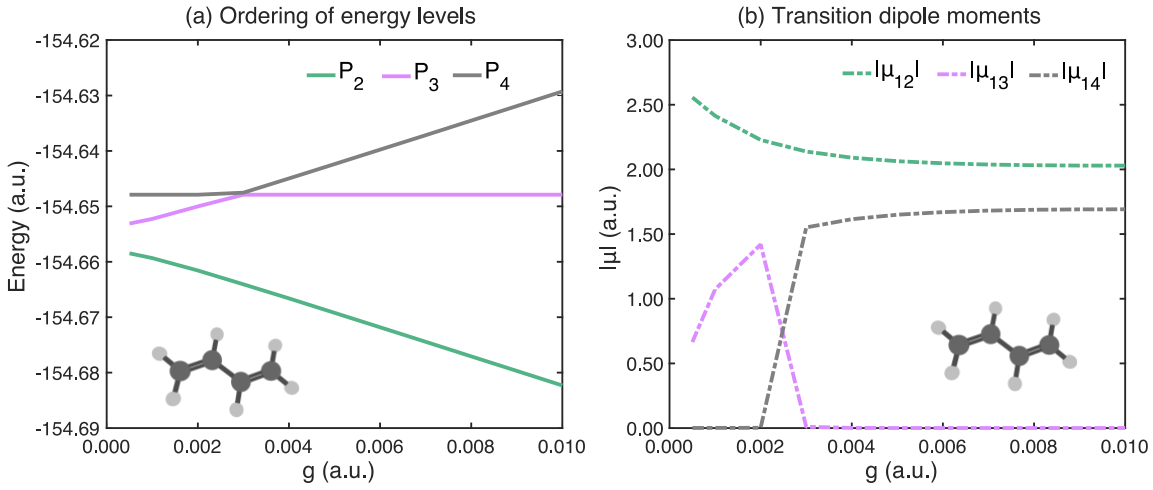

Figure 10. Influence of coupling strength on the energy ordering of the bright and dark states for all trans-butadiene inside an optical cavity. (a) The relative energies of the polaritonic states and (b) the corresponding transition dipole moments are shown at the FC geometry with a three-state polariton model using FOMO-(4,3)-CASCI/6-31G* level of theory.

System	Level of theory	S_1 (osc. Str.) eV (a.u.)	S_2 (osc. Str.) eV (a.u.)	Gap (eV)
all trans-butadiene	Expt.[85]	5.92 (b)	N/A	N/A
	SA3-CAS(4/3)[86]	7.87 (1.08)	7.92 (0.0)	0.05
	SA3-CAS(4/4)-MSPT2[86]	6.34 (0.70)	6.47 (0.0)	0.13
	FOMO-(4,3)-CASCI	7.67 (1.31)	7.95 (0.0)	0.28
all trans-octatetraene	Expt.	3.97 (d)[88]	4.41 (b)[89]	0.44
	NEVPT2-SC(8,8)[87]	4.57 (d)	4.90 (b)	0.33
	FOMO-(4,4)-CASCI	5.79 (0.01)	5.92 (3.97)	0.21
	FOMO-(6,5)-CASCI	5.55 (0.01)	5.76 (4.07)	0.21
OHBA	Expt.[90]	< 3.30 (d)	3.75 (b)	< 0.45
	SA3-CAS(4/3)[84]	4.53 (d)	5.85 (b)	1.32
	SA3-CAS(8/7)[84]	4.50 (d)	4.56 (b)	0.06
	FOMO-(8,7)-CASCI	4.56 (0.03)	4.62 (0.95)	0.06

Table 1. The excitation energies for the first two excited states (S_1 and S_2) and the corresponding gap ($E_{S2} - E_{S1}$) are reported (along with their character) for different levels of theory and experiments. Values which are unavailable are left blank. 'd' and 'b' represent the optically dark and bright states.

https://doi.org/10.26434/chemrxiv-2023-s7s1t **ORCID:** https://orcid.org/0000-0002-8751-7314 Content not peer-reviewed by ChemRxiv. **License:** CC BY-NC-ND 4.0

Before applying the polariton model to such molecules, we tested different active spaces and different Gaussian broadening parameters for the bare molecule with the FOMO-CASCI method to reproduce an energy gap between the two excited states consistent with both the experimental energy gap (if available) and the theoretical gap obtained with more accurate methods. A summary of these tests is shown in Table 1, and on this basis we used an active space of (4,3) for all-*trans* butadiene, (6,5) for all-*trans* octatetraene and (8,7) for o-hydroxybenzaldehyde (OHBA).

When these molecules are investigated inside the optical cavity, a 3-state model generates the polaritonic states for all of them. The cavity-photon is chosen to be resonant with the energy gap corresponding to the optically bright state. The transition dipole moments are computed using FOMO-CASCI and the electromagnetic field polarization unit vector is aligned with the transition dipole of the ground→optically bright transition. The range of coupling strengths is kept in a range that can be generated inside nanoplasmonic antennas (see Table S1). For all-*trans* octatetraene and OHBA, the FC geometries are obtained by performing B3LYP-D3/6-31g* optimizations on S_0. For butadiene, the BLYP/6-31g* optimized S_0 geometry is used.[86]

The state ordering of the 2A (optically dark) and 1B (optically bright) states in butadiene has been a matter of debate, both theoretically and experimentally.[85, 86, 91, 92] Levine and Martínez[86] showed that both state-averaged CASSCF, SA-CAS(4/3), and MSPT2, SA-3-CAS(4/4)-MSPT2, predict the 1B state to lie a bit lower in energy than the 2A state at the Franck-Condon point. We found that FOMO-(4,3)-CASCI with a temperature of 0.35 a.u. reproduces the character of these excited states with a reasonable energy gap. When this molecule is placed inside the cavity, the strongly coupled bright state splits into the LP and UP states and increasing the coupling strength pushes the bright state (LP or P_2) away from the optically dark state (P_4). The variation of the energies of these three states of interest (P_2, P_3, and P_4) for different coupling strengths is shown in Fig. 10a. The transition dipole moments are also plotted in Fig. 10b to track the character of the states. In the bare molecule, the 2A state is observed to cross the 1B state within 20fs. Thus, one can surmise that the cavity effect of pushing the bright state away from the dark state will lengthen the time scale of the 2A/1B crossing.

https://doi.org/10.26434/chemrxiv-2023-s7s1t **ORCID:** https://orcid.org/0000-0002-8751-7314 Content not peer-reviewed by ChemRxiv. **License:** CC BY-NC-ND 4.0

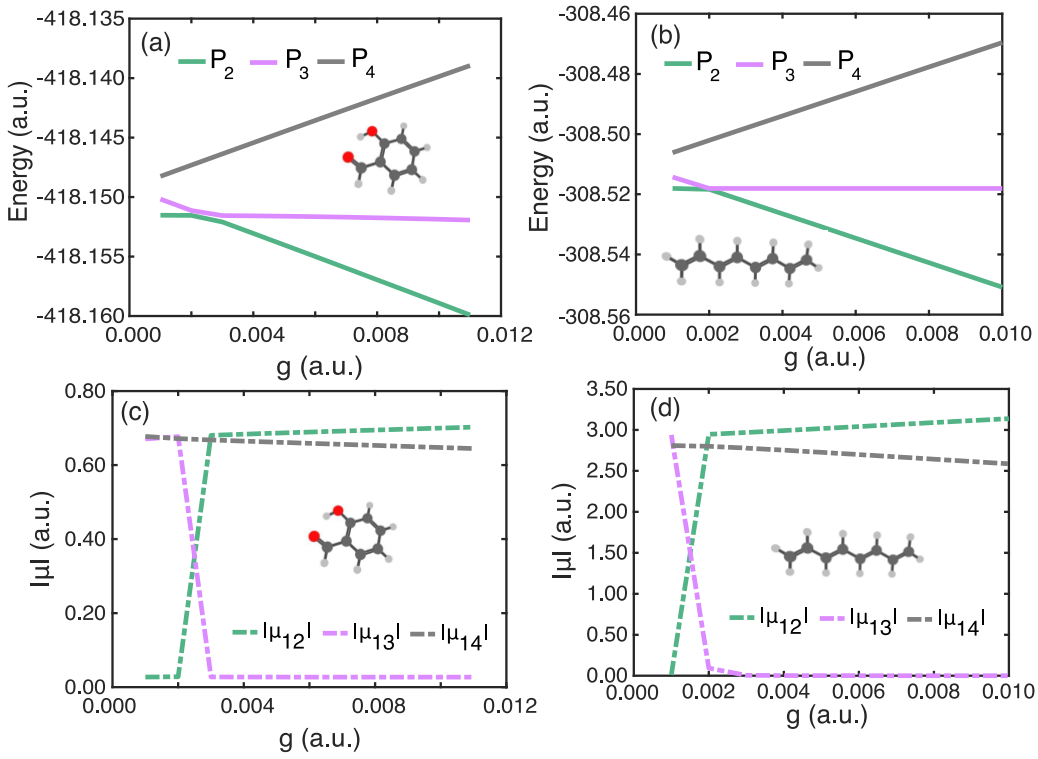

Figure 11. Influence of coupling strength on the energy ordering of the bright and dark states for all trans-octatetraene and OHBA molecules inside an optical cavity are shown at the FC geometry using a three-state polariton model. The variation of energies and their corresponding transition dipole moments for the OHBA molecule are plotted in (a) and (c), respectively, using FOMO-(8,7)-CASCI/6-31G* level of theory. The same for the trans-octatetraene molecule are calculated using FOMO-(6,5)-CASCI/6-31g* level of theory and shown in (b) and (d), respectively.

For octatetraene and OHBA, the optically bright state lies slightly higher in energy than the optically dark state at the FC point. The energy ordering of the important polaritonic states and their corresponding transition dipole moments are shown in Fig. 11. Thus, in these cases, we expect the optically bright state strongly coupled to a cavity photon to cross the optically dark state at some point. Coupling strengths of 0.002 a.u. and 0.003 a.u. are sufficient to bring the bright state below the dark state for all-trans-octatetraene and OHBA molecules, respectively. Such changes in the energy ordering could significantly alter the excited-state dynamics of the trans-octatetraene and OHBA molecules without any direct chemical modifications. Simulations of the excited state dynamics for molecules where the cavity changes bright/dark ordering is an exciting avenue for future studies.

https://doi.org/10.26434/chemrxiv-2023-s7s1t **ORCID:** https://orcid.org/0000-0002-8751-7314 Content not peer-reviewed by ChemRxiv. **License:** CC BY-NC-ND 4.0

IV. Conclusions

In summary, we have developed a first-principles nonadiabatic polariton model to study excited-state dynamics inside an optical cavity. We use a Born-Oppenheimer approximation to decouple the correlated nuclear-photonic-electronic degrees of freedom, but these are recoupled to allow transitions between the states (as in traditional cavity-free nonadiabatic dynamics[93, 94]). We use FOMO-CASCI to generate the electronic wavefunctions. Nonadiabatic dynamics is described with the AIMS method, including transitions between polaritonic states. The quantized quantum field and its interactions with the electronic state are described with a JC-type Hamiltonian, extended to incorporate any number of excited states. The implementation of the FOMO-CASCI analytical gradient and non-adiabatic coupling in the TeraChem package enables us to study the excited-state dynamics in the strong-field regime starting from the strongly coupled polaritonic PES. Although the model is now available with FOMO-CASCI, it can be easily extended to other electronic structure methods, provided analytical gradient, non-adiabatic coupling, and dipole matrix element derivatives are implemented. The initial implementation of this model focused on a single molecule inside the cavity. However, it can be extended to multi-molecule systems using the *ab initio* exciton model,[95-99] exploiting the highly parallelized GPU-based implementation in TeraChem.[95, 99]

As a proof-of-concept application, we applied this model to simulate the excited-state dynamics of salicylideneaniline (SA). Previous studies in the bare SA molecule[81] showed the existence of two competing photo-deactivation pathways, where 80% of the excited state population decays via ESIPT and the rest decays by torsion which blocks the proton transfer. We showed that when this molecule is coupled to a resonant cavity-photon in the strong field regime with experimentally feasible coupling strengths, the branching ratios for ESIPT:torsion can be modified to 95:5 from 80:20. Moreover, detuning the photon energy below resonance can trap the photo-excited SA molecule in the LP state near the FC geometry.

We further extended our applications to a set of molecules (trans-butadiene, trans-octatetraene, and OHBA) with close-lying optically dark/bright states in the FC region. Because there are two close-lying excited states, a three-state polariton model is needed. We show that the gap between the bright and dark states can be increased using feasible coupling strengths. In contrast, for the other two molecules (OHBA and trans-octatetraene), coupling to the cavity changes the ordering of the optically bright and dark states at the FC point. Our results demonstrate

https://doi.org/10.26434/chemrxiv-2023-s7s1t **ORCID:** https://orcid.org/0000-0002-8751-7314 Content not peer-reviewed by ChemRxiv. **License:** CC BY-NC-ND 4.0

that cavity coupling in the strong-field regime can be used to manipulate molecular photochemistry.

Supporting Information

Coordinates for different molecules at the relevant geometries and some additional analysis are included.

Acknowledgements

This material is based upon work supported by the AMOS program of the U. S. Department of Energy, Office of Science, Basic Energy Sciences, Chemical Sciences, Geosciences and Biosciences Division and the DOE Q-Next project.

https://doi.org/10.26434/chemrxiv-2023-s7s1t **ORCID:** https://orcid.org/0000-0002-8751-7314 Content not peer-reviewed by ChemRxiv. **License:** CC BY-NC-ND 4.0

References

1. Brumer, P.; Shapiro, M., Laser control of molecular processes. *Ann. Rev. Phys. Chem.* **1992,** *43*, 257.
2. Dantus, M.; Lozovoy, V. V., Experimental coherent laser control of physicochemical processes. *Chem. Rev.* **2004,** *104*, 1813.
3. Warren, W. S.; Rabitz, H.; Dahleh, M., Coherent control of quantum dynamics: the dream is alive. *Science* **1993,** *259*, 1581.
4. Hutchison, J. A.; Schwartz, T.; Genet, C.; Devaux, E.; Ebbesen, T. W., Modifying chemical landscapes by coupling to vacuum fields. *Ang. Chem. Int. Ed.* **2012,** *51*, 1592.
5. Schwartz, T.; Hutchison, J. A.; Genet, C.; Ebbesen, T. W., Reversible switching of ultrastrong light-molecule coupling. *Phys. Rev. Lett.* **2011,** *106*, 196405.
6. Fontcuberta i Morral, A.; Stellacci, F., Ultrastrong routes to new chemistry. *Nature Mat.* **2012,** *11*, 272.
7. Bandara, H. D.; Cawley, S.; Gascón, J. A.; Burdette, S. C., Short-Circuiting Azobenzene Photoisomerization with Electron-Donating Substituents and Reactivating the Photochemistry with Chemical Modification. *Eur. J. Org. Chem.* **2011,** *2011*, 2916.
8. Becker, Y.; Roth, S.; Scheurer, M.; Jakob, A.; Gacek, D. A.; Walla, P. J.; Dreuw, A.; Wachtveitl, J.; Heckel, A., Selective Modification for Red-Shifted Excitability: A Small Change in Structure, a Huge Change in Photochemistry. *Chem. Eur. J.* **2021,** *27*, 2212.
9. Inoue, Y.; Ikeda, H.; Kaneda, M.; Sumimura, T.; Everitt, S. R.; Wada, T., Entropy-controlled asymmetric photochemistry: switching of product chirality by solvent. *J. Amer. Chem. Soc.* **2000,** *122*, 406.
10. Venkatraman, R. K.; Orr-Ewing, A. J., Solvent effects on ultrafast photochemical pathways. *Acc. Chem. Res.* **2021,** *54*, 4383.
11. Demoulin, B.; Altavilla, S. F.; Rivalta, I.; Garavelli, M., Fine Tuning of Retinal Photoinduced Decay in Solution. *J. Phys. Chem. Lett.* **2017,** *8*, 4407.
12. Pepino, A. J.; Segarra, M., Resolving ultrafast photoinduced deactivations in water-solvated pyrimidine nucleosides. *J. Phys. Chem. Lett.* **2017,** *8*, 1777.
13. Kaluzny, Y.; Goy, P.; Gross, M.; Raimond, J. M.; Haroche, S., Observation of self-induced Rabi oscillations in two-level atoms excited inside a resonant cavity: the ringing regime of superradiance. *Phys. Rev. Lett.* **1983,** *51*, 1175.
14. Thompson, R. J.; Rempe, G.; Kimble, H. J., Observation of normal-mode splitting for an atom in an optical cavity. *Phys. Rev. Lett.* **1992,** *68*, 1132.
15. Garcia-Vidal, F. J.; Ciuti, C.; Ebbesen, T. W., Manipulating matter by strong coupling to vacuum fields. *Science* **2021,** *373*, eabd0336.
16. Chikkaraddy, R.; De Nijs, B.; Benz, F.; Barrow, S. J.; Scherman, O. A.; Rosta, E.; Demetriadou, A.; Fox, P.; Hess, O.; Baumberg, J. J., Single-molecule strong coupling at room temperature in plasmonic nanocavities. *Nature* **2016,** *535*, 127.
17. Flick, J.; Ruggenthaler, M.; Appel, H.; Rubio, A., Atoms and molecules in cavities, from weak to strong coupling in quantum-electrodynamics (QED) chemistry. *Proc. Natl. Acad. Sci.* **2017,** *114*, 3026.
18. Galego, J.; Garcia-Vidal, F. J.; Feist, J., Cavity-induced modifications of molecular structure in the strong-coupling regime. *Phys. Rev. X* **2015,** *5*, 041022.
19. Ribeiro, R. F.; Martinez-Martinez, L. A.; Du, M.; Campos-Gonzalez-Angulo, J.; Yuen-Zhou, J., Polariton chemistry: controlling molecular dynamics with optical cavities. *Chem. Sci.* **2018,** *9*, 6325.

https://doi.org/10.26434/chemrxiv-2023-s7s1t **ORCID:** https://orcid.org/0000-0002-8751-7314 Content not peer-reviewed by ChemRxiv. **License:** CC BY-NC-ND 4.0

20. Mandal, A.; Taylor, M.; Weight, B.; Koessler, E.; Li, X.; Huo, P., Theoretical advances in polariton chemistry and molecular cavity quantum electrodynamics. *Chem. Rev.* **2022,** *123*, 9786.
21. Ruggenthaler, M.; Sidler, D.; Rubio, A., Understanding polaritonic chemistry from ab initio quantum electrodynamics. *Chem. Rev.* **2023,** *in press*.
22. Li, T. E.; Nitzan, A.; Subotnik, J. E., Cavity molecular dynamics simulations of vibrational polariton-enhanced molecular nonlinear absorption. *J. Chem. Phys.* **2021,** *154*, 094124.
23. Li, T. E.; Cui, B.; Subotnik, J. E.; Nitzan, A., Molecular Polaritonics: Chemical Dynamics Under Strong Light-Matter Coupling. *Ann. Rev. Phys. Chem.* **2022,** *73*, 43.
24. Li, T. E.; Nitzan, A.; Subotnik, J. E., Energy-efficient pathway for selectively exciting solute molecules to high vibrational states via solvent vibration-polariton pumping. *Nature Comm.* **2022,** *13*, 1.
25. Li, T. E.; Nitzan, A.; Subotnik, J. E., Collective vibrational strong coupling effects on molecular vibrational relaxation and energy transfer: Numerical insights via cavity molecular dynamics simulations. *Ang. Chem. Int. Ed.* **2021,** *133*, 15661.
26. Li, X.; Mandal, A.; Huo, P., Theory of mode-selective chemistry through polaritonic vibrational strong coupling. *J. Phys. Chem. Lett.* **2021,** *12*, 6974.
27. Li, X.; Mandal, A.; Huo, P., Cavity frequency-dependent theory for vibrational polariton chemistry. *Nature Comm.* **2021,** *12*, 1315.
28. Xiang, B.; Ribeiro, R. F.; Du, M.; Chen, L.; Yang, Z.; Wang, J.; Yuen-Zhou, J.; Xiong, W., Intermolecular vibrational energy transfer enabled by microcavity strong light–matter coupling. *Science* **2020,** *368*, 665.
29. Du, M.; Yuen-Zhou, J., Catalysis by dark states in vibropolaritonic chemistry. *Phys. Rev. Lett.* **2022,** *128*, 096001.
30. Deng, H.; Haug, H.; Yamamoto, Y., Exciton-polariton bose-einstein condensation. *Rev. Mod. Phys.* **2010,** *82*, 1489.
31. Keeling, J.; Kena-Cohen, S., Bose--Einstein condensation of exciton-polaritons in organic microcavities. *Ann. Rev. Phys. Chem.* **2020,** *71*, 435.
32. Fregoni, J.; Granucci, G.; Coccia, E.; Persico, M.; Corni, S., Manipulating azobenzene photoisomerization through strong light--molecule coupling. *Nature Comm.* **2018,** *9*, 1.
33. Csehi, A.; Halász, G. J.; Cederbaum, L. S.; Vibók, Á., Competition between light-induced and intrinsic nonadiabatic phenomena in diatomics. *J. Phys. Chem. Lett.* **2017,** *8*, 1624.
34. Demekhin, P. V.; Cederbaum, L. S., Light-induced conical intersections in polyatomic molecules: General theory, strategies of exploitation, and application. *J. Chem. Phys.* **2013,** *139*, 154314.
35. Kowalewski, M.; Bennett, K.; Mukamel, S., Non-adiabatic dynamics of molecules in optical cavities. *J. Chem. Phys.* **2016,** *144*, 054309.
36. Szidarovszky, T.; Halasz, G. J.; Csaszar, A. G.; Cederbaum, L. S.; Vibok, A., Conical intersections induced by quantum light: Field-dressed spectra from the weak to the ultrastrong coupling regimes. *J. Phys. Chem. Lett.* **2018,** *9*, 6215.
37. Bennett, K.; Kowalewski, M.; Mukamel, S., Novel photochemistry of molecular polaritons in optical cavities. *Faraday Disc.* **2016,** *194*, 259.
38. Feist, J.; Galego, J.; Garcia-Vidal, F. J., Polaritonic chemistry with organic molecules. *ACS Photon.* **2018,** *5*, 205.
39. von den Hoff, P.; Kowalewski, M.; de Vivie-Riedle, R., Searching for pathways involving dressed states in optimal control theory. *Faraday Disc.* **2011,** *153*, 159.

https://doi.org/10.26434/chemrxiv-2023-s7s1t **ORCID:** https://orcid.org/0000-0002-8751-7314 Content not peer-reviewed by ChemRxiv. **License:** CC BY-NC-ND 4.0

40. Kim, J.; Tao, H.; White, J. L.; Petrovic, V. S.; Martinez, T. J.; Bucksbaum, P. H., Control of 1, 3-cyclohexadiene photoisomerization using light-induced conical intersections. *J. Phys. Chem. A* **2012,** *116*, 2758.
41. Kim, J.; Tao, H.; Martinez, T. J.; Bucksbaum, P., Ab initio multiple spawning on laser-dressed states: a study of 1, 3-cyclohexadiene photoisomerization via light-induced conical intersections. *J. Phys. B* **2015,** *48*, 164003.
42. Pritchard, J. D.; Weatherill, K. J.; Adams, C. S., Nonlinear optics using cold Rydberg atoms. In *Annual Review of Cold Atoms and Molecules*, Madison, K. W.; Wang, Y.; Rey, A. M.; Bongs, K., Eds. World Scientific: Singapore, 2013; Vol. 1, pp 301.
43. Jaynes, E. T.; Cummings, F. W., Comparison of quantum and semiclassical radiation theories with application to the beam maser. *Proc. IEEE* **1963,** *51*, 89.
44. Zhang, Y.; Meng, Q.-S.; Zhang, L.; Luo, Y.; Yu, Y.-J.; Yang, B.; Zhang, Y.; Esteban, R.; Aizpurua, J.; Luo, Y.; et al., Sub-nanometre control of the coherent interaction between a single molecule and a plasmonic nanocavity. *Nature Comm.* **2017,** *8*, 1.
45. Hugall, J. T.; Singh, A.; van Hulst, N. F., Plasmonic cavity coupling. *ACS Photon.* **2018,** *5*, 43.
46. Kongsuwan, N.; Demetriadou, A.; Chikkaraddy, R.; Benz, F.; Turek, V. A.; Keyser, U. F.; Baumberg, J. J.; Hess, O., Suppressed quenching and strong-coupling of purcell-enhanced single-molecule emission in plasmonic nanocavities. *ACS Photon.* **2018,** *5*, 186.
47. Wang, D.; Kelkar, H.; Martin-Cano, D.; Utikal, T.; Gotzinger, S.; Sandoghdar, V., Coherent coupling of a single molecule to a scanning Fabry-Perot microcavity. *Phys. Rev. X* **2017,** *7*, 021014.
48. Thomas, A.; George, J.; Shalabney, A.; Dryzhakov, M.; Varma, S. J.; Moran, J.; Chervy, T.; Zhong, X.; Devaux, E.; Genet, C.; et al., Ground-state chemical reactivity under vibrational coupling to the vacuum electromagnetic field. *Ang. Chem. Int. Ed.* **2016,** *128*, 11634.
49. Climent, C.; Galego, J.; Garcia-Vidal, F. J.; Feist, J., Plasmonic Nanocavities Enable Self-Induced Electrostatic Catalysis. *Ang. Chem. Int. Ed.* **2019,** *58*, 8698.
50. Thomas, A.; Lethuillier-Karl, L.; Nagarajan, K.; Vergauwe, R. M. A.; George, J.; Chervy, T.; Shalabney, A.; Devaux, E.; Genet, C.; Moran, J.; et al., Tilting a ground-state reactivity landscape by vibrational strong coupling. *Science* **2019,** *363*, 615.
51. Luk, H. L.; Feist, J.; Toppari, J. J.; Groenhof, G., Multiscale molecular dynamics simulations of polaritonic chemistry. *J. Chem. Theory Comput.* **2017,** *13*, 4324.
52. Vendrell, O., Coherent dynamics in cavity femtochemistry: Application of the multi-configuration time-dependent Hartree method. *Chem. Phys.* **2018,** *509*, 55.
53. Fregoni, J.; Granucci, G.; Persico, M.; Corni, S., Strong coupling with light enhances the photoisomerization quantum yield of azobenzene. *Chem* **2020,** *6*, 250.
54. Herrera, F., Photochemistry with quantum optics from a non-adiabatic quantum trajectory perspective. *Chem* **2020,** *6*, 7.
55. Felicetti, S.; Fregoni, J.; Schnappinger, T.; Reiter, S.; de Vivie-Riedle, R.; Feist, J., Photoprotecting uracil by coupling with lossy nanocavities. *J. Phys. Chem. Lett.* **2020,** *11*, 8810.
56. Antoniou, P.; Suchanek, F.; Varner, J. F.; Foley Iv, J. J., Role of cavity losses on nonadiabatic couplings and dynamics in polaritonic chemistry. *J. Phys. Chem. Lett.* **2020,** *11*, 9063.
57. Sidler, D.; Ruggenthaler, M.; Appel, H.; Rubio, A., Chemistry in quantum cavities: Exact results, the impact of thermal velocities, and modified dissociation. *J. Phys. Chem. Lett.* **2020,** *11*, 7525.

https://doi.org/10.26434/chemrxiv-2023-s7s1t **ORCID:** https://orcid.org/0000-0002-8751-7314 Content not peer-reviewed by ChemRxiv. **License:** CC BY-NC-ND 4.0

58. Kowalewski, M.; Bennett, K.; Mukamel, S., Cavity femtochemistry: Manipulating nonadiabatic dynamics at avoided crossings. *J. Phys. Chem. Lett.* **2016,** *7*, 2050.
59. Fregoni, J.; Garcia-Vidal, F. J.; Feist, J., Theoretical challenges in polaritonic chemistry. *ACS Photon.* **2022,** *9*, 1096.
60. Flick, J.; Appel, H.; Ruggenthaler, M.; Rubio, A., Cavity Born--Oppenheimer approximation for correlated electron--nuclear-photon systems. *J. Chem. Theory Comput.* **2017,** *13*, 1616.
61. Fregoni, J.; Corni, S.; Persico, M.; Granucci, G., Photochemistry in the strong coupling regime: A trajectory surface hopping scheme. *J. Comp. Chem.* **2020,** *41*, 2033.
62. Ruggenthaler, M.; Tancogne-Dejean, N.; Flick, J.; Appel, H.; Rubio, A., From a quantum-electrodynamical light--matter description to novel spectroscopies. *Nature Rev. Chem.* **2018,** *2*, 1.
63. Ruggenthaler, M.; Flick, J.; Pellegrini, C.; Appel, H.; Tokatly, I. V.; Rubio, A., Quantum-electrodynamical density-functional theory: Bridging quantum optics and electronic-structure theory. *Phys. Rev. A* **2014,** *90*, 012508.
64. Flick, J.; Narang, P., Cavity-correlated electron-nuclear dynamics from first principles. *Phys. Rev. Lett.* **2018,** *121*, 113002.
65. Flick, J.; Schäfer, C.; Ruggenthaler, M.; Appel, H.; Rubio, A., Ab initio optimized effective potentials for real molecules in optical cavities: Photon contributions to the molecular ground state. *ACS Photon.* **2018,** *5*, 992.
66. Haugland, T. S.; Ronca, E.; Kjnstad, E. F.; Rubio, A.; Koch, H., Coupled cluster theory for molecular polaritons: Changing ground and excited states. *Phys. Rev. X* **2020,** *10*, 041043.
67. Groenhof, G.; Toppari, J. J., Coherent light harvesting through strong coupling to confined light. *J. Phys. Chem. Lett.* **2018,** *9*, 4848.
68. Zhang, Y.; Nelson, T.; Tretiak, S., Non-adiabatic molecular dynamics of molecules in the presence of strong light-matter interactions. *J. Chem. Phys.* **2019,** *151*, 154109.
69. Li, T. E.; Tao, Z.; Hammes-Schiffer, S., Semiclassical real-time nuclear-electronic orbital dynamics for molecular polaritons: Unified theory of electronic and vibrational strong couplings. *J. Chem. Theory Comput.* **2022,** *18*, 2774.
70. Slavicek, P.; Martinez, T. J., Ab initio floating occupation molecular orbital-complete active space configuration interaction: An efficient approximation to CASSCF. *J. Chem. Phys.* **2010,** *132*, 234102.
71. Ben-Nun, M.; Quenneville, J.; Martinez, T. J., Ab initio multiple spawning: Photochemistry from first principles quantum molecular dynamics. *J. Phys. Chem. A* **2000,** *104*, 5161.
72. Kim, M.-K.; Sim, H.; Yoon, S. J.; Gong, S.-H.; Ahn, C. W.; Cho, Y.-H.; Lee, Y.-H., Squeezing photons into a point-like space. *Nano Lett.* **2015,** *15*, 4102.
73. Hohenstein, E. G.; Bouduban, M. E. F.; Song, C.; Luehr, N.; Ufimtsev, I. S.; Martinez, T. J., Analytic first derivatives of floating occupation molecular orbital-complete active space configuration interaction on graphical processing units. *J. Chem. Phys.* **2015,** *143*, 014111.
74. Hohenstein, E. G., Analytic formulation of derivative coupling vectors for complete active space configuration interaction wavefunctions with floating occupation molecular orbitals. *J. Chem. Phys.* **2016,** *145*, 174110.
75. Seritan, S.; Bannwarth, C.; Fales, B. S.; Hohenstein, E. G.; Isborn, C. M.; Kokkila-Schumacher, S. I. L.; Li, X.; Liu, F.; Luehr, N.; Snyder Jr, J. W.; et al., TeraChem: A graphical processing unit-accelerated electronic structure package for large-scale ab initio molecular dynamics. *WIReS: Comp. Mol. Sci.* **2021,** *11*, e1494.

https://doi.org/10.26434/chemrxiv-2023-s7s1t **ORCID:** https://orcid.org/0000-0002-8751-7314 Content not peer-reviewed by ChemRxiv. **License:** CC BY-NC-ND 4.0

76. Okabe, C.; Nakabayashi, T.; Inokuchi, Y.; Nishi, N.; Sekiya, H., Ultrafast excited-state dynamics in photochromic N-salicylideneaniline studied by femtosecond time-resolved REMPI spectroscopy. *J. Chem. Phys.* **2004,** *121*, 9436.
77. Avadanei, M.; Kus, N.; Cozan, V.; Fausto, R., Structure and photochemistry of N-salicylidene-p-carboxyaniline isolated in solid argon. *J. Phys. Chem. A* **2015,** *119*, 9121.
78. Sekikawa, T.; Schalk, O.; Wu, G.; Boguslavskiy, A. E.; Stolow, A., Initial processes of proton transfer in salicylideneaniline studied by time-resolved photoelectron spectroscopy. *J. Phys. Chem. A* **2013,** *117*, 2971.
79. Spörkel, L.; Cui, G.; Thiel, W., Photodynamics of schiff base salicylideneaniline: trajectory surface-hopping simulations. *J. Phys. Chem. A* **2013,** *117*, 4574.
80. Ortiz-Sánchez, J. M.; Gelabert, R.; Moreno, M.; Lluch, J. M., Electronic-structure and quantum dynamical study of the photochromism of the aromatic Schiff base salicylideneaniline. *J. Chem. Phys.* **2008,** *129*.
81. Pijeau, S.; Foster, D.; Hohenstein, E. G., Effect of nonplanarity on excited-state proton transfer and internal conversion in salicylideneaniline. *J. Phys. Chem. A* **2018,** *122*, 5555.
82. Pijeau, S.; Hohenstein, E. G., Improved complete active space configuration interaction energies with a simple correction from density functional theory. *J. Chem. Theory Comput.* **2017,** *13*, 1130.
83. Coe, J. D.; Levine, B. G.; Martinez, T. J., Ab initio molecular dynamics of excited-state intramolecular proton transfer using multireference perturbation theory. *J. Phys. Chem. A* **2007,** *111*, 11302.
84. Coe, J. D.; J. Martinez, T., Ab initio multiple spawning dynamics of excited state intramolecular proton transfer: the role of spectroscopically dark states. *Mol. Phys.* **2008,** *106*, 537.
85. Doering, J. P.; McDiarmid, R., Electron impact study of the energy levels of trans-1, 3-butadiene: II. Detailed analysis of valence and Rydberg transitions. *J. Chem. Phys.* **1980,** *73*, 3617.
86. Levine, B. G.; Martinez, T. J., Ab initio multiple spawning dynamics of excited butadiene: Role of charge transfer. *J. Phys. Chem. A* **2009,** *113*, 12815.
87. Ronca, E.; Angeli, C.; Belpassi, L.; De Angelis, F.; Tarantelli, F.; Pastore, M., Density relaxation in time-dependent density functional theory: Combining relaxed density natural orbitals and multireference perturbation theories for an improved description of excited states. *J. Chem. Theory Comput.* **2014,** *10*, 4014.
88. Hudson, B. S.; Kohler, B. E.; Schulten, K., Linear Polyene Electronic Structure and Potential Surfaces. In *Excited States*, Lim, E. C., Ed. Academic: New York, 1982; Vol. 6, p 3.
89. Heimbrook, L. A.; Kohler, B. E.; Levy, I. J., Fluorescence from the 1 1 B u state of trans, trans-1, 3, 5, 7-octatetraene in a free jet. *J. Chem. Phys.* **1984,** *81*, 1592.
90. Morgan, M. A.; Orton, E.; Pimentel, G. C., Characterization of ground and electronically excited states of o-hydroxybenzaldehyde and its non-hydrogen-bonded photorotamer in 12 K rare gas matrixes. *J. Phys. Chem.* **1990,** *94*, 7927.
91. Watson, M. A.; Chan, G. K., Excited States of Butadiene to Chemical Accuracy: Reconciling Theory and Experiment. *J. Chem. Theory Comput.* **2012,** *8*, 4013.
92. Chadwick, R. R.; Gerrity, D. P.; Hudson, B. S., Resonance Raman spectroscopy of butadiene: Demonstration of a 2 1Ag state below the 1 1Bu V state. *Chem. Phys. Lett.* **1985,** *115*, 24.
93. Crespo-Otero, R.; Barbatti, M., Recent Advances and Perspectives on Nonadiabatic Mixed Quantum-Classical Dynamics. *Chem. Rev.* **2018,** *118*, 7026.
94. Curchod, B. F. E.; Martinez, T. J., Ab Initio Nonadiabatic Quantum Molecular Dynamics. *Chem. Rev.* **2018,** *118*, 3305.

https://doi.org/10.26434/chemrxiv-2023-s7s1t **ORCID:** https://orcid.org/0000-0002-8751-7314 Content not peer-reviewed by ChemRxiv. **License:** CC BY-NC-ND 4.0

95. Sisto, A.; Glowacki, D. R.; Martinez, T. J., Ab initio nonadiabatic dynamics of multichromophore complexes: A scalable graphical-processing-unit-accelerated exciton framework. *Acc. Chem. Res.* **2014,** *47*, 2857.
96. Sisto, A.; Stross, C.; van der Kamp, M. W.; O'Connor, M.; McIntosh-Smith, S.; Johnson, G. T.; Hohenstein, E. G.; Manby, F. R.; Glowacki, D. R.; Martinez, T. J., Atomistic non-adiabatic dynamics of the LH2 complex with a GPU-accelerated ab initio exciton model. *Phys. Chem. Chem. Phys.* **2017,** *19*, 14924.
97. Morrison, A. F.; Herbert, J. M., Low-Scaling Quantum Chemistry Approach to Excited-State Properties via an ab Initio Exciton Model: Application to Excitation Energy Transfer in a Self-Assembled Nanotube. *J. Phys. Chem. Lett.* **2015,** *6*, 4390.
98. Li, X.; Parrish, R. M.; Liu, F.; Kokkila-Schumacher, S. I. L.; Martinez, T. J., An Ab Initio Exciton Model Including Charge-Transfer Excited States. *J. Chem. Theory Comput.* **2017,** *13*, 3493.
99. Li, X.; Parrish, R. M.; Martinez, T. J., An ab initio exciton model for singlet fission. *J. Chem. Phys.* **2020,** *153*, 184116.

https://doi.org/10.26434/chemrxiv-2023-s7s1t **ORCID:** https://orcid.org/0000-0002-8751-7314 Content not peer-reviewed by ChemRxiv. **License:** CC BY-NC-ND 4.0